Optimization Approach for Multi-domain Optical Network Provisioning

K. Liang, M. Rahnamay-Naeini, H. M. K. Alazemi, N. Min-Allah, M. Peng, and N. Ghani

***Abstract*—Multi-domain optical network provisioning is a key focus area as users continue to demand scalable bandwidth services across wider network regions. To date, a range of distributed schemes have been proposed to achieve lightpath routing across domain boundaries. In general, these solutions rely upon hierarchical routing and provisioning strategies and are mostly heuristics based. As such, it is difficult to gauge their true load-carrying capacity and effectiveness. Hence in order to address this concern, this effort proposes a formal optimization-based model for multi-domain lightpath setup pursuant to several key objectives, i.e., including throughput maximization, resource minimization, and load balancing. This model is then solved for some sample network topologies, and the results are compared versus existing heuristic strategies.**

***Index Terms*—Multi-domain lightpath provisioning; Multi-domain optical networks; Optimization.**

I. Introduction

Optical *wavelength division multiplexing* (WDM) technologies have evolved to provide very high levels of bandwidth scalability over base fiber-optic substrates. Hence many backbone operators have extensively deployed WDM networking transport and switching systems to offer new bandwidth services for their clients. Now as WDM networks become increasingly prevalent, there is a pressing need to interconnect and provision services across *multiple* optical networking domains, i.e., as delineated by geographic regions, technology types, administrative ownership, etc. [1,2]. In particular, many applications in the scientific computing realm are readily dependent upon such offerings to support massive data transfers across extended global regions; see [3].

Overall the topic of multi-domain WDM network provisioning has received notable attention in recent years; see surveys in [1,2]. Here most of the proposed *routing and wavelength* (RWA) solutions have outlined distributed provisioning strategies, as it is quite difficult (if not impossible) for a single entity to maintain "global network" topology and resource information across all domains, i.e., due to obvious scalability and inter-region privacy concerns. Furthermore, many of these strategies leverage from related inter-domain/inter-area routing concepts in ubiquitous packet-switching networks. For example, early schemes have proposed path-vector strategies to allow border gateway *optical cross-connect* (OXC) nodes to maintain "next-hop" information to other domains [4]. Meanwhile others have proposed detailed hierarchical routing strategies in which border OXC nodes use topology aggregation to propagate abstract wavelength/converter state, i.e., link-state routing [5–7]. This information is then used to compute "end-to-end" skeleton routes across domains for further expansion via distributed signaling protocols. Finally, recent efforts have also studied decentralized (per-domain) lightpath computation using recursive backward computation/signaling techniques; see [8,9].

In general, the above solutions are mostly heuristics-based and use graph-theoretic path computation at the intra- and inter-domain levels. Moreover, these schemes operate with delayed (path-vector, link-state) information, resulting in reduced provisioning effectiveness, e.g., in terms of blocking performance and resource efficiency [10,11]. As such, it is difficult to ascertain the true achievable performance of hierarchical provisioning strategies. Now many optical networking studies have used optimization-based algorithms to bound RWA performance under idealized conditions with full *a priori* knowledge of requests and network topologies; see [12–14]. However, these schemes are only applicable to *single-domain* settings owing to their assumptions on the global network state. As such, further use of optimization-based methods for multi-domain lightpath provisioning has not been considered. Along these lines, this paper proposes a novel optimization model for hierarchical multi-domain RWA pursuant to several objectives, e.g., throughput maximization, resource minimization, and load balancing. The key aim here is to develop a reference framework against which to gauge the performance of distributed multi-domain heuristics.

Overall, this paper is organized as follows. First, Section II presents a survey of some recent work in multi-domain optical network provisioning. Subsequently, Section III presents a detailed optimization model for multi-domain lightpath RWA, and its solution approach

Manuscript received September 11, 2013; accepted September 20, 2013; published November 27, 2013 (Doc. ID 197314).

K. Liang and M. Rahnamay-Naeini are with the University of New Mexico, 1 University Boulevard NE, Albuquerque, New Mexico 87131, USA.

H. M. K. Alazemi is with Kuwait University, Kuwait City, Kuwait.

N. Min-Allah is with the COMSATS Institute of Information Technology, Islamabad, Pakistan, and the Computer Science and Artificial Intelligence Laboratory (CSAIL) at the Massachusetts Institute of Technology, Boston, Massachusetts, USA.

M. Peng is with Wuhan University, Wuchang, Wuhan, Hubei, China.

N. Ghani (e-mail: nghani@usf.edu) is with the University of South Florida, 4202 E. Fowler Avenue, Tampa, Florida 33620, USA.

http://dx.doi.org/10.1364/JOCN.5.001413

is then detailed in Section IV, i.e., including inter- and intra-domain optimizations. An existing multi-domain heuristic scheme is then briefly reviewed in Section V for comparison purposes, and its performance is analyzed versus the proposed optimization scheme in Section VI for several network topologies. Conclusions and future work directions are then presented in Section VII.

II. Background

Multi-domain lightpath provisioning is a challenging problem as scalability and privacy concerns limit the type of information that can be exchanged between domains. As a result, network practitioners and researchers have developed a range of *distributed* strategies to implement an end-to-end lightpath setup; see surveys in [1,2]. These solutions run *hierarchical* routing protocols to establish partial state visibility across domains. This information is then used to perform distributed end-to-end route computation, e.g., by computing routes in a skeleton or incremental manner and "expanding" them via inter-domain signaling. Alternatively, others have also looked at more decentralized solutions that do not require hierarchical routing provisions. For the most part, all of these various optical multi-domain RWA solutions have their origins in related frameworks for packet/frame-switching data networks, i.e., including link-state and path-vector routing. A review of some of these schemes is now presented; see also summary in Table I.

A. Hierarchical Routing/Provisioning Schemes

In link-state routing, network nodes generate update messages to notify each other about changes in the status/resources of their attached links. This dissemination allows all nodes to build and maintain their own link-state topology and resource databases and thereby make independent provisioning decisions. Now when applying this concept at the hierarchical inter-domain level, the associated border gateway nodes usually run another (higher) level of link-state routing between themselves to disseminate the *inter-domain* link state. This distribution allows gateways to maintain inter-domain databases with "global" connectivity information between domains, i.e., skeleton views. Topology abstraction is also widely used here to generate condensed "abstract" representations of the domain-internal state. This approach transforms physical domain topologies into smaller resource graphs with fewer abstract nodes/links and was originally proposed for packet-switching networks to help summarize bandwidth and delay information, e.g., simple node, star, tree, and full-mesh abstractions; see [2] and [10,11]. For example, simple node abstraction reduces a domain to a single (weighted) vertex and represents the highest level of summarization. Meanwhile the other schemes reduce a domain to its respective border nodes interconnected via appropriate star, tree, or full-mesh topologies, i.e., with $O(N)$, $O(N)$, and $O(N^2)$ abstract links, respectively. Leveraging this, researchers have also proposed hierarchical routing schemes for multi-domain optical networks.

TABLE I
Summary of Multi-domain Optical Network Provisioning Research

Reference	Summary
[5,6]	Hierarchical link-state routing with full-mesh topology abstraction
[7,17,18]	Hierarchical link-state routing with full-mesh topology abstraction (opto-electronic conversion)
[15]	Hierarchical link-state routing with simple node abstraction (opto-electronic conversion)
[19–22]	Hierarchical distance/path-vector routing
[8,9]	Per-domain provisioning using backward recursive path computation (BRPC)

In one of the first studies on hierarchical routing for all-optical WDM networks [5], the authors develop novel topology aggregation algorithms to condense wavelength and delay information on path routes between border nodes. A relative update triggering policy is also used to disseminate state information across domain boundaries along with *loose route* (LR) computation and signaling expansion schemes. Further provisions are also added in the LR computation to handle inaccurate (summarized) state information, i.e., via bypass links. Simulations show good reduction in inter-domain routing overheads, but blocking performance still lags behind an idealized "flat" routing solution, i.e., a single idealized provisioning entity with fully accurate global domain state. Meanwhile, [6] also studies all-optical multi-domain RWA using simple node and full-mesh topology abstraction. The latter approach uses abstract links to summarize domain-traversing wavelength information. Graph-theoretic *k-shortest path* (k-SP) algorithms are then used to compute/select skeleton path LRs to achieve load balancing. Signaling expansion is also done using the ubiquitous *resource reservation* (RSVP) protocol. The overall findings show notably lower blocking with full-mesh abstraction as well as lower signaling overheads. However, inter-domain routing overheads are several factors higher and increase with the number of border nodes.

In general, most real-world multi-domain networks use opto-electronic wavelength conversion/regeneration at domain boundaries to ensure bit-level user *service level agreements* (SLAs), especially in inter-carrier settings [2]. Moreover, extended multi-domain distances will also mandate increased signal regeneration. Hence studies have also looked at opto-electronic conversion at border gateways. For example, [15] studies lightpath routing with full conversion at border OXC nodes and outlines three heuristic schemes (assuming simple node abstraction). The first baseline solution computes end-to-end routes over a "flat" global topology and serves as an idealized reference. Meanwhile, the second approach computes skeleton paths with the shortest (inter-domain) hop counts in the skeleton graph. Finally, the third solution performs "domain-to-domain" segment expansion along a fixed sequence of domains, akin to the "per-domain" PCE computation [16]. Several gateway selection strategies are also proposed to

handle multiple border nodes, including random, closest-distance, and least-loaded selection. Results show that the hierarchical skeleton path scheme gives the lowest blocking and is closely matched by domain segment expansion.

However, the opto-electronic multi-domain RWA schemes in [15] only compute fixed routes and do not incorporate any "active" link-load information. To address this limitation, [7] presents a more dynamic solution that uses a modified full-mesh abstraction scheme based upon the most congested subpaths between border nodes. Skeleton path computation is also done using "load-based" weights to minimize wavelength/converter usages on critical links and nodes. Overall, the findings here show the lowest blocking and setup signaling overheads with full-mesh abstraction, i.e., as compared to simple node abstraction without any domain-level converter state information. The results also indicate that sparse opto-electronic conversion at domain boundaries (coupled with full-mesh topology abstraction) gives sizeable blocking reduction versus full opto-electronic conversion and simple node abstraction. Nevertheless, full-mesh abstraction schemes pose notable scalability challenges as they have high routing overheads and require shorter inter-domain routing update intervals [2,17]. Hence some specialized update policies have also been proposed to limit routing overheads, e.g., partial advertising [17] and gradient-based triggering [18].

Now earlier, some researchers also proposed hierarchical distance/path-vector routing for multi-domain lightpath provisioning. In particular, these schemes leverage the *border gateway protocol* (BGP) for inter-autonomous system provisioning between Internet domains and add new extensions for lightpath routing/wavelength assignment. For example, the *"optical" BGP* (O-BGP) scheme [4] augments BGP reachability update messages (containing path routes to other domains) to include the wavelength availability state. Meanwhile [19] presents another WDM path-vector routing scheme that advertises *multiple* routes to a destination domain, each based upon different constraints. A two-phase backward reservation protocol is also defined to achieve fast setup, leveraging from standardized RSVP signaling. However, none of the above studies conduct any performance evaluation of their proposed designs, e.g., in terms of blocking, resource utilization, etc. However, subsequent work in [20] and [21] does present a more detailed performance analysis of path-vector routing in multi-domain WDM networks. In particular, here the authors use adaptive filtering techniques to first estimate the number of available wavelengths on each destination domain path. Distributed signaling methods are then proposed to expand intra-domain routes along these end-to-end paths, and simulations show good blocking reduction versus (fixed) shortest-path selection. Finally, another study in [22] also proposes a distance-vector solution that maintains several alternate "next-hop" routes to destination domains and uses a distributed scheme to concatenate domain sequences and build end-to-end lightpath routes. Analog signal impairment concerns are also addressed in the expansion phase to limit *bit error rate* (BER) degradation for end-to-end routes.

B. Decentralized Provisioning Schemes

Alternatively, some designers have studied more decentralized multi-domain RWA schemes based upon the *path computation element* (PCE) framework [16]. This standard defines dedicated PCE entities for each domain and allows them to interact in a distributed manner to compute and expand inter-domain routes, e.g., via *PCE communication protocol* (PCEP) signaling [23]. Now one of the most notable schemes here is the *backward recursive path computation* (BRPC) algorithm [24,25], which computes a reverse-spanning tree from the destination to the source domain. Although originally defined for bandwidth-routing networks, further adaptations of this solution have also been developed for optical WDM networks; see [8,9]. However, BRPC-based schemes generally assume fixed (precomputed) "end-to-end" domain sequences and hence do not operate with much inter-domain visibility. Instead, the main focus is on resolving intra-domain routes and performing gateway node selection along these skeleton routes. As such these strategies will give suboptimal performance under dynamic conditions with varying load conditions on inter-domain links.

C. Open Issues

In summary, most of the above-detailed multi-domain lightpath provisioning studies have only looked at distributed heuristics-based strategies. Therefore it is quite difficult to gauge the true effectiveness of these schemes in terms of carried loads or resource efficiencies. Indeed, there is a clear need to develop more formalized models to bound/quantify the achievable performance of hierarchical multi-domain lightpath RWA strategies, e.g., under idealized conditions with *a priori* demands. Along these lines, this paper presents a detailed optimization-based model for multi-domain lightpath provisioning. This solution is then solved for some sample topologies, and its performance is compared against some advanced multi-domain heuristic strategies. To the best of our knowledge, this is the first such study on optimization in (optical) hierarchical multi-domain networks.

III. Optimization Model

A novel *integer linear programming* (ILP) optimization model is now presented for multi-domain lightpath provisioning. This formulation assumes full *a priori* knowledge of multi-domain user requests and mimics the overall hierarchical routing and provisioning process via a two-step optimization process; see Fig. 1. Namely, skeleton path sequences are first derived for all requests over a global abstract topology subject to specific traffic engineering objectives and constraints. This abstract topology uses full-mesh abstraction to condense domains as a mesh of links between their respective border nodes. Next, the individual domain-traversing lightpath segments (subpaths) are extracted from the skeleton paths and then optimized over

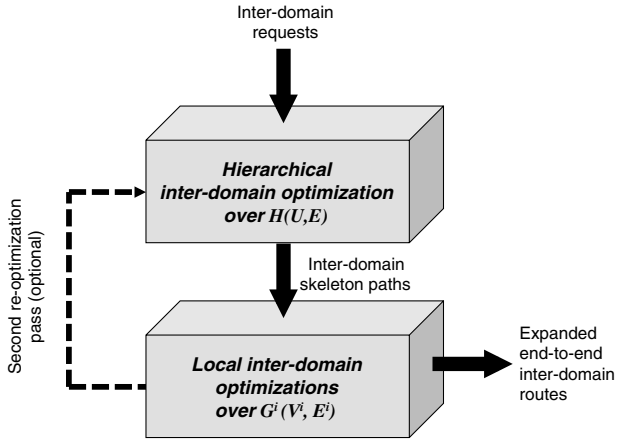

Fig. 1. Two-step multi-domain optimization solution.

their respective local domain topologies. Now in order to model realistic settings here, it is assumed that all domains are transparent (i.e., all-optical) but support full opto-electronic wavelength conversion at their border gateway OXC nodes. Indeed, similar considerations have also been made in other studies [7,15] owing to the increased distances (signal degradation) across multiple domains and the need for bit-level SLA monitoring at boundary nodes. The requisite notation is now introduced followed by the detailed optimization objectives and constraints.

A. Notation Overview

Consider a multi-domain WDM network with D domains, with the ith domain having n^i nodes and b^i border nodes, $1 \le i \le D$. Here each ith domain is represented by a subgraph, $\boldsymbol{G}^i(\boldsymbol{V}^i, \boldsymbol{L}^i)$, where $\boldsymbol{V}^i = \{v_1^i, v_2^i, \ldots, v_n^i\}$ are the physical domain OXC nodes and $\boldsymbol{L}^i = \{l_{km}^{ii}\}$ are the physical intra-domain links; i.e., l_{km}^{ii} is the link between OXC nodes v_k^i and v_m^i $(1 \le i \le D, 1 \le k, m \le n^i)$. All intra-domain links are assumed to be bidirectional with maximum wavelength capacity C_1. In addition, the border OXC nodes in domain i are also denoted by the set $\boldsymbol{B}^i \subseteq V^i$, i.e., where $|\boldsymbol{B}^i| = b^i$.

Now assuming hierarchical multi-domain routing with full-mesh abstraction, an associated "higher-level" *abstract* topology is defined comprising all border OXC nodes and their interconnecting physical (inter-domain) and abstract (intra-domain) links. This topology is represented by the graph $\boldsymbol{H}(\boldsymbol{U}, \boldsymbol{E})$, where $\boldsymbol{U} = \sum_i \{\boldsymbol{B}^i\}$ is the global set of border nodes and $\boldsymbol{E}$ is the global set of links, i.e., $\boldsymbol{E} = \boldsymbol{E}_{\text{phy}} \cup \sum_i \boldsymbol{E}_{\text{mesh}}^i$, where $\boldsymbol{E}_{\text{phy}}$ is the set of physical inter-domain links and $\boldsymbol{E}_{\text{mesh}}^i$ is the set of abstract intra-domain links for domain i $(1 \le i \le D)$. Specifically, $\boldsymbol{E}_{\text{phy}} = \{e_{km}^{ij}\}$, where e_{km}^{ij} is the physical link interconnecting OXC node v_k^i in domain i with OXC node v_m^j in domain j $(1 \le i, j \le D, 1 \le k \le b^i, 1 \le m \le b^j)$. Without loss of generality, it is also assumed that all inter-domain links in $\boldsymbol{E}_{\text{phy}}$ have maximum wavelength capacity C_2. Meanwhile, the abstract link set for domain i is given by $\boldsymbol{E}_{\text{mesh}}^i = \{e_{jk}^{ii}\}$, where e_{jk}^{ii} is the abstract link between border nodes v_j^i and v_k^i and $|\boldsymbol{E}_{\text{mesh}}^i| = b^i(b^i - 1)$ $(1 \le i \le D,\ 1 \le j, k \le b^i)$.

A sample abstract graph, $\boldsymbol{H}(\boldsymbol{U}, \boldsymbol{E})$, for a three-domain network topology is shown in Fig. 2. Here, topology abstraction reduces the physical topology for domain 2, $\boldsymbol{G}^2(\boldsymbol{V}^2, \boldsymbol{L}^2)$, to a full-mesh subgraph consisting of three border nodes (v_1^2, v_2^2, v_3^2) and six abstract links (e_{12}^{22}, e_{21}^{22}, e_{13}^{22}, e_{31}^{22}, e_{23}^{22}, e_{32}^{22}).

B. Objectives and Constraints

As mentioned earlier, the proposed solution (Fig. 1) applies optimization at both the inter- and intra-domain topology levels, i.e., over the graphs $\boldsymbol{H}(\boldsymbol{U}, \boldsymbol{E})$ and $\boldsymbol{G}^i(\boldsymbol{V}^i, \boldsymbol{L}^i)$, respectively. Now at the inter-domain level, the assumption of full opto-electronic conversion at border OXC nodes obviates the need for wavelength selection on skeleton routes; i.e., only path selection is required. Meanwhile, at the intra-domain level, the proposed formulation decouples lightpath route computation from wavelength selection. Namely, an ILP optimization is first used to compute the intra-domain route segments, and then an appropriate wavelength selection policy is used to assign the wavelengths, i.e., akin to other (single-domain) RWA studies in [12,13,26–28]. As a result, similar traffic engineering objectives can be pursued at each level, i.e., global inter-domain and local intra-domain, and hence only the inter-domain optimization model is presented here for brevity's sake, i.e., for abstract graph $\boldsymbol{H}(\boldsymbol{U}, \boldsymbol{E})$.

Consider an *a priori* set of user lightpath demands, denoted by the set ot 3-tuples $\{(s_n, d_n, r_n)\}$, where n represents the request index, s_n is the source OXC node, d_n is the destination OXC node, and r_n is the number of required wavelengths, i.e., $s_n \in \boldsymbol{V}^i$, $d_n \in \boldsymbol{V}^j$, and $i \ne j$. Also, let f_n denote the number of wavelengths allocated to the nth request, x_{km}^{nij} denote the number of wavelengths routed over link e_{km}^{ij} for request n, and α denote the *maximum link utilization* (MLU) allowed, i.e., in order to prevent link saturation. Furthermore, without loss of generality, assume that all links in $\boldsymbol{H}(\boldsymbol{U}, \boldsymbol{E})$ have capacity $c_{ij} = C_2$.

Using these variables, a multi-objective function, $\boldsymbol{F}$, is defined to pursue several objectives across the full batch of input user requests:

$$\text{Max}\, \boldsymbol{F} = w_1 \sum_{n \in N} f_n - w_2 \sum_{n \in N} \sum_{l_{km}^{ij} \in E} x_{km}^{nij} - w_3 \alpha, \tag{1}$$

where w_1, w_2, and w_3 are fractional weighting factors that sum to unity, i.e., $w_1 + w_2 + w_3 = 1$, and

$$F_1 = \sum_{n \in N} f_n, \tag{2a}$$

$$F_2 = -\sum_{n \in N} \sum_{(i,j) \in E} x_{ij}^n, \tag{2b}$$

$$F_3 = -\alpha, \tag{2c}$$

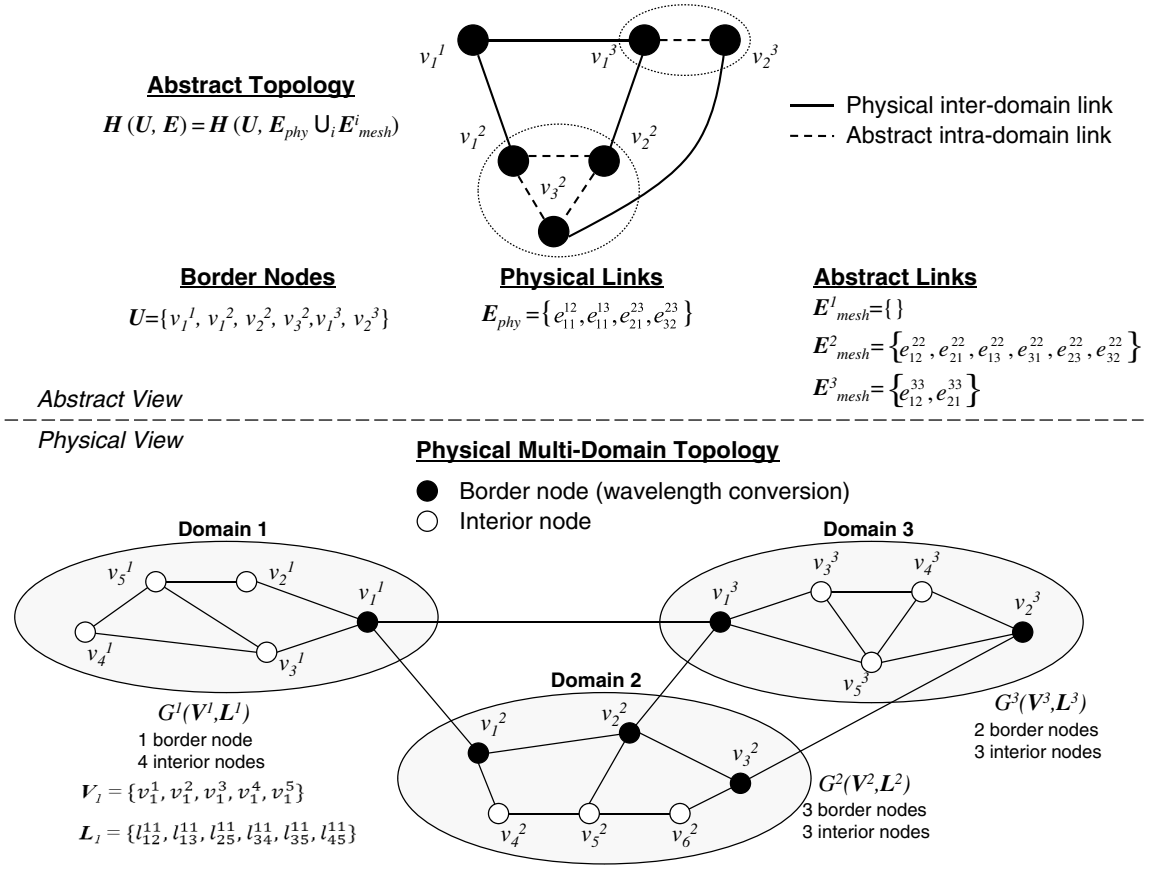

Fig. 2. Full-mesh topology abstraction and notation overview.

subject to the following constraints:

$$\sum_{(j,m):l_{km}^{ij}\in E} x_{km}^{nij} - \sum_{(j,m):l_{mk}^{ji}\in E} x_{mk}^{nji} = \begin{cases} f_n; & \text{if } v_k^i = s_n \\ -f_n; & \text{if } v_k^i = d_n, \\ 0; & \text{otherwise} \end{cases} \quad (3)$$

$$\sum_{n\in N} x_{km}^{nij} \le \alpha C_2; \qquad l_{km}^{ij} \in E, \quad (4)$$

$$f_n \le r_n; \qquad n \in N, \quad (5)$$

$$x_{km}^{nij} \in \{0, 1, 2, \ldots\}; \qquad n \in N, l_{km}^{ij} \in E, \quad (6)$$

$$f_n \in \{0, 1, 2, \ldots, r_n\}; \qquad n \in N, l_{km}^{ij} \in E, \quad (7)$$

$$0 \le \alpha \le 1. \quad (8)$$

Overall, F comprises three parts and is similar to the objective function proposed in [27] for single-domain WDM networks (and is shown to give improved load balancing and decreased resource consumption). The key aim here is to achieve a weighted balance between maximizing aggregate throughput, minimizing resource consumption, and achieving load balancing. Namely, Eq. (2a) represents the total throughput for the given requests and network topology, Eq. (2b) represents the negative of total resource consumption, and Eq. (2c) is the negative of MLU. Meanwhile Eqs. (3)–(8) specify the model constraints. Specifically, Eq. (3) represents a flow constraint between the incoming and outgoing flows at each (border) node in the abstract graph. Meanwhile, Eq. (4) restricts the total *relative* traffic carried on a link to below the MLU value, i.e., less than αC_2. Also, Eq. (5) ensures that the number of allocated wavelengths is less than the number of requested wavelengths for each request. Finally, Eqs. (6) and (7) represent integrality constraints, and Eq. (8) restricts the MLU for all links to be below α. Note that this optimization model directly incorporates load balancing via the F_3 term and also Eq. (8). In particular, the solution tries to route all lightpath requests in a batch (simultaneous) manner so as to try to balance traffic distribution across all links and not exceed the prespecified (static) MLU value. The ILP solution approach is now presented.

IV. Solution Approach

As mentioned in Section III, the ILP model is solved in a "top-down" manner by first optimizing skeleton

inter-domain routes for all requests over $\boldsymbol{H}(\boldsymbol{U},\boldsymbol{E})$. These routes are then used to identify the traversed abstract links, from which the required "all-optical" intra-domain requests are generated to drive the second optimization step, i.e., solving ILP formulations for the individual subgraphs $\boldsymbol{G}^i(\boldsymbol{V}^i,\boldsymbol{L}^i)$ (see Section IV.B). Subsequently, the entire end-to-end lightpaths are resolved by concatenating all intra-domain segments (with the same flow index) with their respective inter-domain links in $\boldsymbol{H}(\boldsymbol{U},\boldsymbol{E})$. Without loss of generality, it can be assumed that all multi-domain lightpath requests are for one wavelength, i.e., $r_n = 1$. Overall, this two-step optimization approach is much more feasible as it is difficult (impossible) to solve a single ILP formulation for a very large "flat" single-domain network comprising all domain nodes and links, i.e., the idealized case of global state. To the best of our knowledge, this is the first such application of optimization for the hierarchical inter-domain RWA problem. Consider the details here.

A. Hierarchical Inter-domain Optimization

Consider the case of skeleton route optimization over the global abstract topology, $\boldsymbol{H}(\boldsymbol{U},\boldsymbol{E})$. Since this topology represents a "domain-level" summary of the entire network, it is reasonable to assume that this problem can be be solved on a standard workstation computer. Hence assuming a valid solution here, the computed number of unit flows (wavelengths) routed along on each *physical* inter-domain link and *abstract* intra-domain link can be determined. Specifically, let the outputted (computed) values for x_{km}^{nij} be denoted by $X_{km}^{nij} = \{0,1\}$, i.e., due to single-wavelength request assumption ($r_n = 1$). Using these values, the number of requests routed on any given (inter-domain physical or intra-domain abstract) link can be determined by simply summing up the X_{km}^{nij} values over all requests, i.e., $X_{km}^{ij} = \sum_{n\in N} X_{km}^{nij}$.

Now for the case of abstract links, i.e., $i = j$, the total number of wavelengths routed over link e_{km}^{ii} is equivalent to the number of "local" intra-domain (subpath) requests that must be routed between ingress border node v_k^i and egress border node v_m^i in domain i. Hence these requests can be grouped into the set $\{(v_k^i, v_m^i, 1)\}$ for domain i and then used to drive the second stage of the optimization, detailed next in Section IV.B. Carefully note that the above numbering scheme assigns the same request indices to

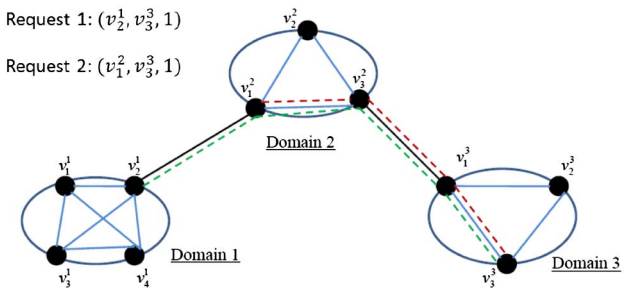

Fig. 3. Inter-domain skeleton path routing for sample three-domain network.

TABLE II
INTRA-DOMAIN REQUESTS

	Domain 1	Domain 2	Domain 3
Request 1	—	$(v_1^2, v_3^2, 1)$	$(v_1^3, v_3^3, 1)$
Request 2	—	$(v_2^2, v_3^2, 1)$	$(v_1^3, v_3^3, 1)$

the local domain requests as those for the corresponding inter-domain requests, essentially matching which "end-to-end" lightpath each subpath request belongs to. Indeed, this is possible due to the assumption of single-wavelength requests, i.e., as the optimization solution may otherwise yield multiple routes for multi-wavelength requests.

An example of hierarchical skeleton path computation and subpath request generation is also shown for the sample three-domain network in Fig. 3. In particular, there are two multi-domain lightpath requests that need to be routed here, request 1 $(v_2^1, v_3^3, 1)$ and request 3 $(v_2^2, v_3^3, 1)$. Now assuming that the ILP solution returns valid skeleton paths over $\boldsymbol{H}(\boldsymbol{U},\boldsymbol{E})$ for both requests, the associated skeleton paths are shown in Fig. 3 via dashed colored lines, i.e., $e_{21}^{12} - e_{13}^{22} - e_{31}^{23} - e_{13}^{33}$ (for request 1) and $e_{23}^{22} - e_{31}^{23} - e_{12}^{33}$ (for request 2). From these sequences, the associated intra-domain subpath requests can also be generated for each domain, as shown in Table II.

B. Local Intra-domain Optimization

The second optimization phase takes the subpath requests generated from the skeleton paths and attempts to provision (domain-traversing) lightpaths over the individual domain topologies. In particular, intra-domain route selection is done using the same optimization formulation in Section III.B, i.e., by applying it over the local domain topology, $\boldsymbol{G}^i(\boldsymbol{V}^i,\boldsymbol{L}^i)$. Now once the local subpath routes have been resolved, wavelength selection is done in order to ensure wavelength continuity across all-optical domains. In particular, the *most-used* (MU) wavelength assignment strategy is used here as it shown to give good results in both single- and multi-domain networks; see [6,12]. If, however, an available wavelength cannot be found for a particular subpath, then the lightpath request for that particular index is dropped (failed). Finally, once all intra-domain wavelengths have been assigned, the complete "end-to-end" multi-domain lightpath route can be generated. This is done for each request index by concatenating the physical links on its inter-domain skeleton route with the expanded intra-domain subpath routes with the same request index. As wavelength selection on inter-domain links is not an issue, i.e., due to full opto-electronic conversion at gateway OXC nodes, any available wavelength can be selected here. The overall pseudocode description of this two-stage ILP solution is also given in Fig. 4.

C. Optional Reoptimization Pass

Carefully note that special cases may arise if requests traversing two (or more) common domains fail the

1: Given domain-level sub-graphs, $\boldsymbol{G}^i(\boldsymbol{V}^i, \boldsymbol{L}^i)$, intra-domain link sets, $\boldsymbol{E}_{phy}$, and a priori multi-domain lightpath request set, $\{(s_n, d_n, r_n)\}$.
2: Generate full-mesh topology abstractions for each domain and construct abstract graph $\boldsymbol{H}(\boldsymbol{U}, \boldsymbol{E})$.
3: Run first-level ILP optimization to compute skeleton loose routes over $\boldsymbol{H}(\boldsymbol{U}, \boldsymbol{E})$ to maximize multi-objective function, i.e., F [Eq. (1)].
4: Extract intra-domain traversing segments on successful skeleton paths (above) and generate intra-domain sub-path request sets for each domain i, $\{(v_k^i, v_m^i, 1)\}$.
5: Run second-level ILP optimizations over all domain sub-graphs, $\boldsymbol{G}^i(\boldsymbol{V}^i, \boldsymbol{L}^i)$, to compute domain-traversing segments. Perform *most used* (MU) wavelength selection for successful sub-paths.
6: Concatenate successful domain-traversing segments to generate complete "end-to-end" lightpath sequences.

Fig. 4. Pseudocode for two-stage ILP solution (single-pass only).

optimization setup at *different* domains. These scenarios can result in multiple requests being denied even if there are available resources to support at least some of them. Hence in order to improve setup success rates, a second optional "reoptimization" step is added, i.e., depicted via the dashed line in Fig. 1. Namely, the goal here is to prune (i.e., deliberately fail) some of the "overlapping" requests in order to allow others to be successful. This is perhaps best shown via an example in Fig. 5, where request 1 (from v_2^1 to v_3^3) overlaps with request 2 (from v_1^2 to v_3^3) at domains 2 and 3. Now both requests experience blocking, with request 1 failing at domain 3 and request 2 failing at domain 2; i.e., intra-domain optimization cannot find wavelength-continuous subpaths. However, a slight resource reassignment can allow at least one of these requests to be successful. Specifically, if the two failed domain subpaths in Fig. 5 are both assigned to request 1, then request 2 can be routed across domain 2, i.e., *without* changing the total number of wavelengths used in the original assignment.

The reoptimization procedure is formally detailed now and tries to reallocate resources between failed requests traversing one or more common domains (but experiencing

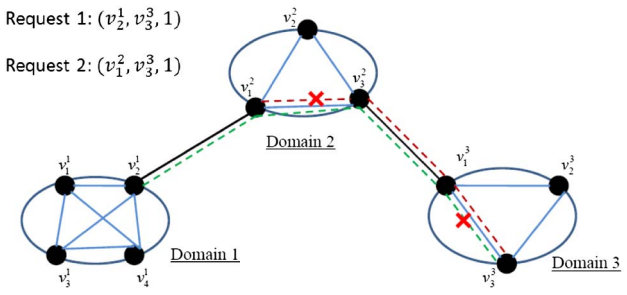

Fig. 5. Overlapping inter-domain requests failing setup at different domains.

blocking at different domains). Carefully note that since there can be multiple overlaps between the skeleton routes, in turn there can be many potential combinations for pruning failed skeleton routes; i.e., this can be treated as an optimization problem itself. However, to simplify matters here a different strategy is used. Namely, the two-stage optimization is rerun with the capacities of the abstract links in $\boldsymbol{H}(\boldsymbol{U}, \boldsymbol{E})$ set to the number of *successful* traversing intra-domain routes between the respective border nodes, i.e., X_{km}^{ij} as obtained from the first pass of the optimization (Section IV.A). This approach ensures that the number of resources used at the inter-domain level is the same as that computed in the initial optimization.

V. Referrence Heuristic Scheme

As per Section II, most existing multi-domain RWA schemes use graph-based heuristics. Along these lines, an advanced hierarchical routing solution from [7] is chosen here for comparison purposes. This scheme computes full-mesh topology abstractions to summarize intra-domain wavelength resource state information between border nodes, i.e., via "abstract" links. Namely, the exact set of available wavelengths on an abstract link is computed by searching the k-shortest paths between the respective border node pair and selecting the path with the maximum number of free wavelengths. The abstract link's wavelength availability vector is then determined by AND-ing the individual binary wavelength availability vectors of all physical intra-domain links on the selected route. Next, abstract link entities are advertised between border nodes as part of a hierarchical routing process in conjunction with updates for *physical* inter-domain links. Namely, a relative change triggering strategy is used to generate these updates, i.e., if the change in wavelength resources exceeds a *significance change factor* (SCF) and the time since the last update exceeds a *hold-down* (HT) timer; see [6,7] for details.

Overall, inter-domain routing dissemination allows domain PCE systems to maintain global topology databases with active "aggregated" network state. This information is then used to field incoming lightpath requests and compute associated skeleton LR sequences over the abstract topology, i.e., by using either hop-count or load-based metrics [7]. Finally, these resultant path sequences are fully expanded using inter-PCE signaling via the PCE protocol [23], i.e., with each intermediate domain PCE computing a local domain-traversing segment between the specified ingress/egress border nodes in the skeleton route; see [7] for complete details.

VI. Performance Evaluation

The multi-domain optimization solution is now tested and also compared against the distributed heuristic scheme in [7] (as overviewed in Section V). Here two different topologies are used, including a smaller-sized six-domain network as well as a larger 16-domain network (reflective of a national backbone). In particular, the former

topology is shown in Fig. 6, and has an average domain size of seven nodes and nine bidirectional inter-domain links. Meanwhile, the 16-domain network is a modification of the NSFNET backbone topology that replaces all of the nodes with domains; see Fig. 7. Here the individual domain sizes are varied between 7 and 10 nodes and there are a total of 25 bidirectional inter-domain links.

The ILP model in Section III is specified using the PuLP package, which is a Python-based linear programming modeler. This formulation is then solved hierarchically (as explained in Section IV) using the *GNU Linear Programming Kit* (GLPK) for a randomly generated set of multi-domain requests, i.e., uniform random source and destination domains and uniform random nodes within these domains. Furthermore, the weights for the objective function [Eq. (1)] are set to $\{w_1, w_2, w_3\} = \{0.9, 0.05, 0.05\}$. In general, these values emphasize throughput maximization but also try to reduce resource consumption by assigning a nonzero weight to F_2, i.e., to account for the generally higher cost of bandwidth usage on inter-domain links. In addition, load balancing is also taken into account by assigning a nonzero weight to F_3.

Meanwhile, the multi-domain hierarchical routing heuristic scheme (outlined in Section V) is analyzed using custom-developed *OPNET Modeler* discrete-event simulation models. Here, the inter-domain routing update thresholds are set to SCF = 0.1 (10%) and the corresponding HT timers to 120 s, i.e., 20% of the average connection holding time. Furthermore, in order to ensure a fair comparison between the optimization and heuristics-based strategies, the same randomly generated set of lightpath requests is tested for each particular input "load" point, i.e., measured by the number of requests. All incoming requests are also given infinite holding times in order to compare the findings with those from the hierarchical ILP solution, i.e., no departures. However, since the order of these input requests can affect the resulting route selection and success rates for the heuristic scheme, the input sequences are randomly shuffled to generate 10 different variations, and the best results are taken for comparison with the ILP model. The detailed findings are now presented.

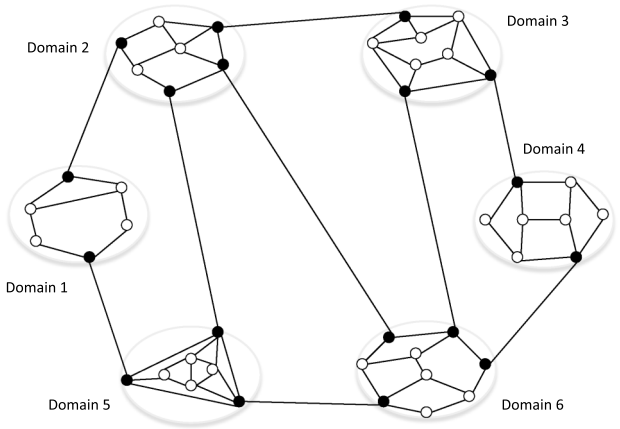

Fig. 6. Six-domain network topology.

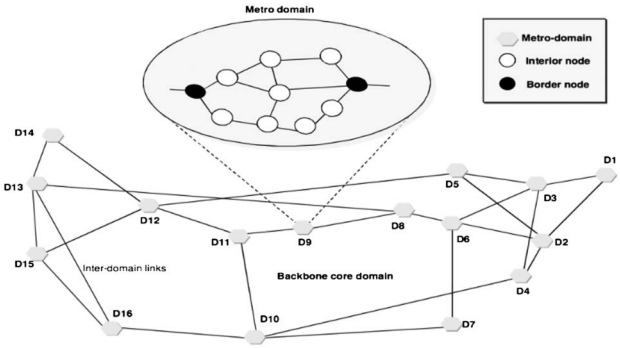

Fig. 7. Modified 16-domain NSFNET topology.

Initial tests are done for the six-domain network for two different intra-/inter-domain link sizes, i.e., $C_1, C_2 = 8, 16$ wavelengths, respectively. Here both the (single-pass) optimization and (double-pass) reoptimization schemes are tested, and the overall setup success rates for varying input request sizes (input loads) are plotted in Fig. 8. Overall, these results indicate relatively close performance between the ILP and (hierarchical routing) heuristic schemes at very low input load regimes for $C_1 = C_2 = 16$. However, as loads increase to moderate levels, the heuristic scheme tends to saturate around a certain number of successful connections, whereas the ILP schemes continue to improve. For example, the ILP solutions give well more than two times the success rate of the heuristic strategy at high input loads. In addition, these results also show very little (no) improvement with the optional ILP reoptimization step for this smaller topology.

Next, the corresponding average hop counts are measured and plotted in Fig. 9 for successful lightpath setups. For the most part, these values indicate declining trends with increased load, and this is expected as higher contention levels generally result in increased failure rates for longer paths. The optional reoptimization pass also yields little change in the average hop count. Now carefully note that these results exhibit higher variability at lower loads due to the reduced request (sample) sizes. As a result, the

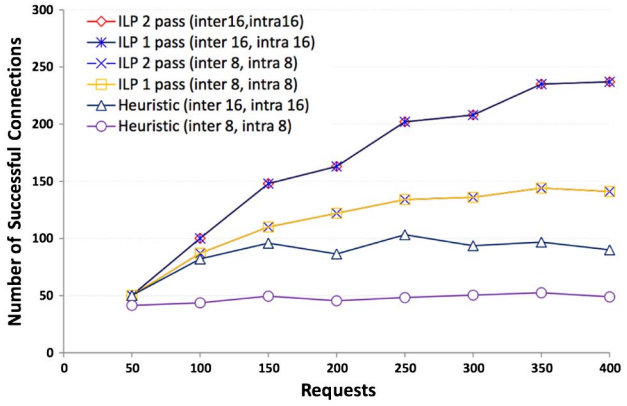

Fig. 8. Successful requests, six-domain (C_1, $C_2 = 8$ and C_1, $C_2 = 16$).

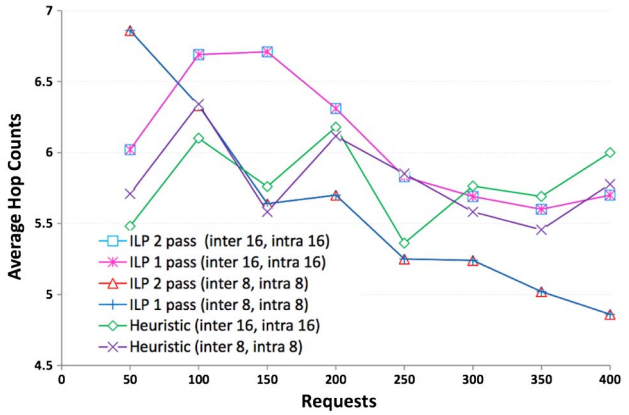

Fig. 9. Average hop count, six-domain (C_1, $C_2 = 8$ and C_1, $C_2 = 16$).

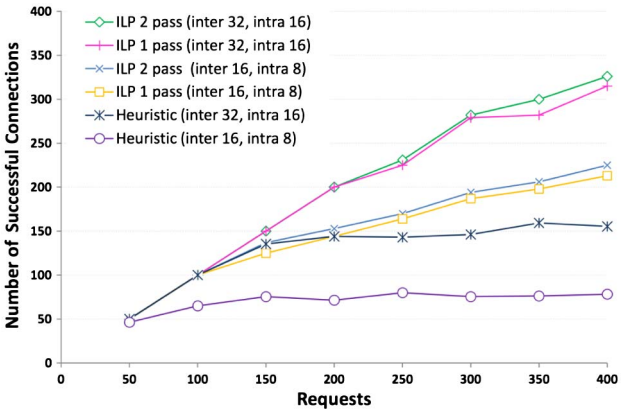

Fig. 11. Successful requests, six-domain ($C_2 = 2C_1 = 16$ and $C_2 = 2C_1 = 32$).

batch sizes may not be uniformly distributed and have significantly more (less) long (short) path connections. However, as the batch sizes increase, this variability reduces notably. Furthermore, averaging the results over more runs (than the 10 currently done) will also help reduce this variability. The overall run times for the different optimization steps are also shown in Fig. 10 for the smaller C_1, $C_2 = 8$ wavelength scenario and indicate superlinear growth. As expected, hierarchical optimization (over abstract skeleton graph) yields the lowest overheads as run times are dominated by the intra-domain optimizations.

Additional tests are also done for the six-domain scenario with differing intra- and inter-domain link sizes. Namely, the number of inter-domain link wavelengths is set to double the number of intra-domain wavelengths in order to model more realistic network scenarios with increased inter-domain trunk sizes, i.e., $C_2 = 2C_1$. The associated lightpath setup success rates here are plotted in Fig. 11 for varying request sizes and show similar behaviors to the equivalent-link scenario for varying input loads. For example, for $C_1 = 8$ and $C_2 = 16$, the ILP-based schemes closely track the hierarchical routing heuristics to about 150 requests, i.e., low-medium load regime, but then give much better performance at higher loads, i.e., more than 200% gain in setup success rates. Furthermore, unlike earlier results for equivalent intra-/inter-domain link sizes, the second reoptimization step does yield some slight improvement in setup success rates, i.e., about 3%–5% less blocking at higher loads. Meanwhile, the average hop-count values are also shown in Fig. 12 and generally follow a declining trend. However, the ILP-based schemes yield slightly higher lightpath resource consumption, i.e., as they are more successful at finding longer routes at higher load/congestion.

The larger 16-domain modified NSFNET topology is tested next for both the optimization and heuristics-based approaches. Here Fig. 13 plots the number of successful setup requests for this network with two different intra- and inter-domain link sizes, i.e., 8 and 16 wavelengths. Again, these results reconfirm earlier findings with the six-domain network, with the optimization strategies giving well more than twice the number of successful lightpath setups at higher loads. In addition, the optional "reoptimization" pass tends to yield little reduction in blocking. The corresponding average hop counts are also plotted in Fig. 14 and show a more definitive downward

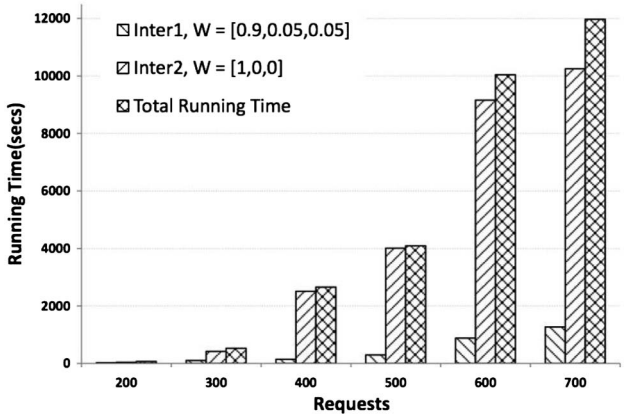

Fig. 10. Sample ILP run times for 16-domain network (C_1, $C_2 = 8$).

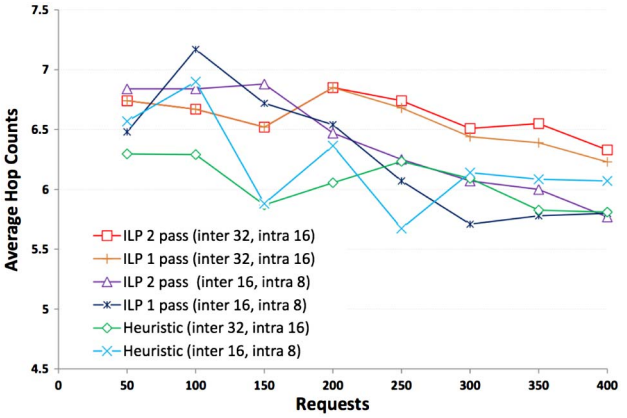

Fig. 12. Average hop count, six-domain ($C_2 = 2C_1 = 16$ and $C_2 = 2C_1 = 32$).

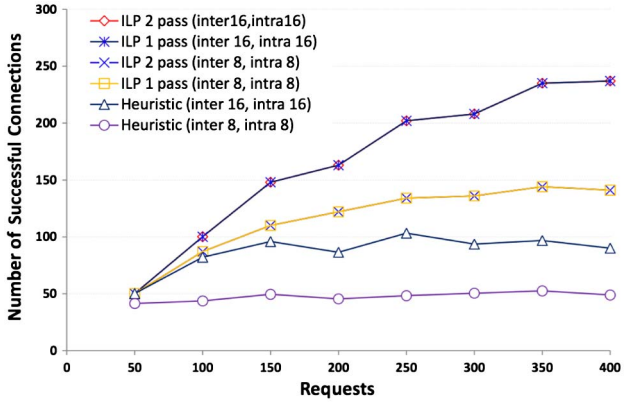

Fig. 13. Successful requests, 16-domain (C_1, $C_2 = 8$ and C_1, $C_2 = 16$).

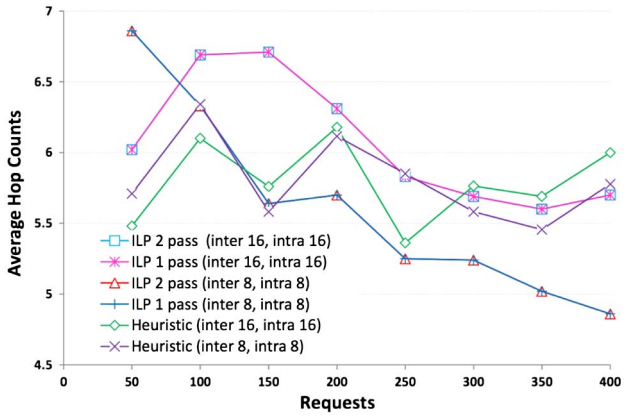

Fig. 14. Average hop count, 16-domain (C_1, $C_2 = 8$ and C_1, $C_2 = 16$).

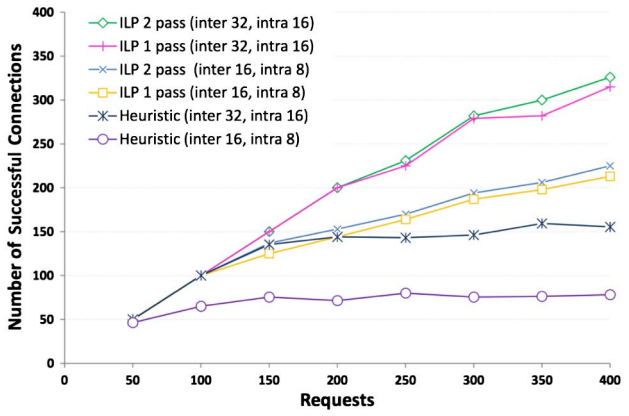

Fig. 15. Successful requests ($C_2 = 2C_1 = 16$ and $C_2 = 2C_1 = 32$).

trend with increasing input loads for both the ILP and heuristic schemes, i.e., about 30% lower at extremely high loads. In general, this behavior is expected as increased loads will drive up link utilization and lower the probability of finding longer domain-traversing subpath routes

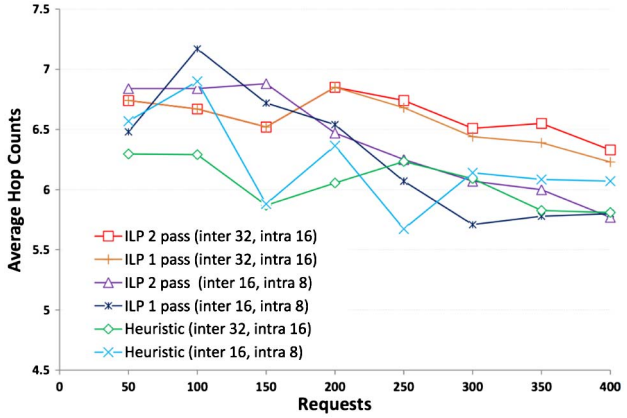

Fig. 16. Average hop count ($C_2 = 2C_1 = 16$ and $C_2 = 2C_1 = 32$).

with free (and continuous) wavelength channels. Moreover, the ILP objective function in Eq. (1) also takes into account resource usage, and hence this will also try to minimize the number of links used.

Now careful analysis of the optimization results for the 16-domain topology indicates very few setup failures in the second intra-domain ILP step. In other words, for equivalent sized intra-/inter-domain link scenarios, nearly all blocking tends to occur due to *inter-domain link* congestion. As a result, further tests are with larger inter-domain links in order to reflect more realistic operator link sizing strategies, i.e., $C_2 = 2C_1$. Along these lines, Fig. 15 plots the number of successful setups and Fig. 16 plots the corresponding average hop-count values for this modified scenario. Again, these findings indicate much better blocking performance with the ILP-based strategies, yielding between 2 and 3 times more successful setups at medium-to-high loads. As per similar runs with the six-domain network, slight blocking reduction is also observed with the optional reoptimization pass, in the range of about 3%.

VII. Conclusion

This paper presented an optimization-based study of lightpath routing in multi-domain optical networks. In particular, the hierarchical routing/provisioning framework was modeled by developing objectives to capture throughput, resource utilization, and load balancing at both the inter-domain (skeleton graph) and intra-domain (local graph) levels. A solution was then presented to solve this formulation by using a two-step approach that applies optimization at the global "abstract" inter-domain level as well as the local intra-domain level. The proposed scheme was then tested using sample multi-domain network topologies, and its results were compared against those with an advanced distributed heuristic scheme (using link-state routing and skeleton path computation/expansion). Overall, detailed findings show much-improved performance with the proposed optimization approach, yielding several factors improvement (reduction) in setup success (request blocking) rates. As such, this work provides an invaluable

reference against which to gauge the performance of distributed multi-domain optical lightpath provisioning schemes. Future efforts will look at developing improved heuristic strategies to reduce the performance gap with the optimization-based benchmarks developed herein. In addition, other efforts will also look at expanding the optimization model to incorporate lightpath protection under single and multiple failures. In particular, the latter pertain to scenarios with highly correlated and cascading outages, as triggered by large-scale catastrophic events.

Acknowledgments

This work has been funded by the Defense Threat Reduction Agency (DTRA) under the Basic Research Program (Award No. HDTRA1-09-1-0026). The authors are very grateful to this agency for its generous support.

References

[1] M. Chamania and A. Jukan, "A survey of inter-domain peering and provisioning solutions for the next generation optical networks," *IEEE Commun. Surv. Tutorials*, vol. 11, no. 1, pp. 33–51, Mar. 2009.

[2] N. Ghani, M. Peng, and A. Rayes, "Provisioning and survivability in multi-domain optical networks," in *WDM Systems and Networks*, A. Neophytos, G. Ellinas, and I. Roudas, Eds. New York: Springer, 2012, pp. 481–519.

[3] T. Lehman, X. Yang, N. Ghani, F. Gu, C. Guok, I. Monga, and B. Tierney, "Multilayer networks: An architecture framework," *IEEE Commun. Mag.*, vol. 49, no. 5, pp. 122–130, May 2011.

[4] B. S. Arnaud, M. Weir, and J. Coulter, "BGP optical switches and lightpath route arbiter," *Opt. Networks Mag.*, vol. 2, no. 2, pp. 73–81, Mar./Apr. 2001.

[5] S. Sanchez-Lopez, X. Masip-Bruin, E. Marin-Tordera, and J. Sole-Pareta, "A hierarchical routing approach for GMPLS-based control plane for ASON," in *IEEE Int. Conf. on Communications (ICC)*, Seoul, South Korea, June 2005.

[6] Q. Liu, M. A. Kok, N. Ghani, and A. Gumaste, "Hierarchical routing in multi-domain optical networks," *Comput. Commun.*, vol. 30, no. 1, pp. 122–131, Dec. 2006.

[7] Q. Liu, N. Ghani, N. Rao, A. Gumaste, and M. Garcia, "Distributed inter-domain lightpath provisioning in the presence of wavelength conversion," *Comput. Commun.*, vol. 30, no. 18, pp. 3362–3375, Dec. 2007.

[8] Y. Zhao, J. Zhang, Y. Ji, and W. Gu, "Routing and wavelength assignment problem in PCE-based wavelength-switched optical networks," *J. Opt. Commun. Netw.*, vol. 2, no. 4, pp. 196–205, Apr. 2010.

[9] R. Casellas, R. Martinez, R. Munoz, and S. Gunreben, "Enhanced backwards recursive path computation for multi-area wavelength switched optical networks under wavelength continuity constraint," in *IEEE/OSA OFC*, San Diego, CA, Mar. 2009.

[10] F. Hao and E. Zegura, "On scalable QoS routing: Performance evaluation of topology aggregation," in *IEEE INFOCOM*, Tel Aviv, Israel, Mar. 2003.

[11] T. Korkmaz and M. Krunz, "Source-oriented topology aggregation with multiple QoS parameters in hierarchical networks," *ACM Trans. Model. Comput. Simul.*, vol. 10, no. 4, pp. 295–325, Oct. 2000.

[12] H. Zang, J. Jue, and B. Mukherjee, "A review of routing and wavelength assignment approaches for wavelength-routed optical WDM networks," *Opt. Networks Mag.*, vol. 1, no. 1, pp. 47–60, Jan. 2000.

[13] R. Ramaswami and K. Sivarajan, "Routing and wavelength assignment in all-optical networks," *IEEE/ACM Trans. Netw.*, vol. 3, no. 5, pp. 489–500, Oct. 1999.

[14] K. Christodoulopoulos, K. Manousakis, and E. Varvarigos, "Comparison of routing and wavelength assignment algorithms in WDM networks," in *IEEE Global Communications Conf. (GLOBECOM)*, New Orleans, LA, Dec. 2008.

[15] Y. Zhu, A. Jukan, and M. Ammar, "Multi-segment wavelength routing in large-scale optical networks," in *IEEE Int. Conf. on Communications (ICC)*, Anchorage, AK, May 2003.

[16] A. Farrel, J. Vasseur, and J. Ash, "A path computation element (PCE)- based architecture," IETF RFC 4655, Aug. 2006.

[17] Y. Yu, Y. Jin, W. Sun, W. Guo, and W. Hu, "On the efficiency of inter-domain state advertising in multi-domain networks," in *IEEE Global Communications Conf. (GLOBECOM)*, Honolulu, HI, Nov. 2009.

[18] Q. Liu, C. Xie, T. Frangieh, N. Ghani, A. Gumaste, and N. Rao, "Routing scalability in multi-domain DWDM networks," *Photonic Network Commun.*, vol. 17, no. 1, pp. 63–74, 2009.

[19] O. Yu, "Intercarrier interdomain control plane for global optical networks," in *IEEE ICC*, New York City, NY, June 2004.

[20] M. Yannuzzi, X. Masip-Bruin, S. Sanchez-Lopez, and E. Tordera, "Interdomain RWA based on stochastic estimation methods and adaptive filtering for optical networks," in *IEEE Global Communications Conf. (GLOBECOM)*, San Francisco, CA, Nov. 2006.

[21] M. Yannuzzi, X. Masip-Bruin, G. Fabrego, and S. Sanchez-Lopez, "Toward a new route control model for multi-domain optical networks," *IEEE Commun. Mag.*, vol. 46, no. 6, pp. 104–111, June 2008.

[22] X. Yang and B. Ramamurthy, "Inter-domain dynamic routing in multi-layer optical transport networks," in *IEEE Global Communications Conf. (GLOBECOM)*, San Francisco, CA, Dec. 2003.

[23] A. Farrel, A. Satyanarayana, A. Iwata, N. Fujita, and G. Ash, "Crankback signaling extensions for MPLS and GMPLS RSVP-TE," IETF RFC 4920, July 2007.

[24] J. Vasseur, R. Zhang, N. Bitar, and J. L. Roux, "A backward recursive PCE-based computation (BRPC) procedure to compute shortest constrained inter-domain traffic engineered label switched paths," IETF RFC 5441, Apr. 2009.

[25] S. Dasgupta, J. De Oliveira, and J. Vasseur, "Path-computation-element-based architecture for interdomain MPLS/GMPLS traffic engineering: Overview and performance," *IEEE Network*, vol. 21, no. 4, pp. 38–45, July/Aug. 2007.

[26] D. Banerjee and B. Mukherjee, "Wavelength-routed optical networks: Linear formulation resource budgeting tradeoffs, and a reconfiguration study," *IEEE/ACM Trans. Netw.*, vol. 8, no. 5, pp. 598–607, May 2000.

[27] J. Crichigno, W. Shu, and M. Wu, "Throughput optimization and traffic engineering in WDM networks considering multiple metrics," in *IEEE Int. Conf. on Communications (ICC)*, Cape Town, South Africa, June 2010.

[28] J. Crichigno, J. Khoury, W. Shu, M. Wu, and N. Ghani, "Dynamic routing optimization in WDM networks," in *IEEE Global Communications Conf. (GLOBECOM)*, Miami, FL, Dec. 2010.

Kaile Liang received her B.Sc and Masters degrees in telecommunication engineering from the Beijing University of Posts and Telecommunications (BUPT). She then joined the Electrical and Computer Engineering (ECE) Department at the University of New Mexico under the supervision of Prof. Ghani and completed her Ph.D. degree in July 2012. She is currently working as a Software Engineer (Quality) at eBay, and her research interests include network optimization, performance analysis, simulation, and software defined networking/network virtualization.

Mahshid Rahnamay-Naeini received her B.Sc in computer engineering from Sharif University of Technology in 2007 and her M.Sc in computer engineering with concentration on computer networks from Amirkabir University of Technology (Tehran Polytechnic) in 2009. She is currently an electrical engineering (communication systems) Ph.D. candidate in the Electrical and Computer Engineering Department at the University of New Mexico. Her research interests include reliability and performance analysis of communication networks, smart power grids, smart-grid networking, data centers and cloud computing, resource management, and stochastic modeling.

Hamed M. K. Alazemi received the B.Sc. and M.S. degrees in electrical engineering from Washington University, St. Louis, MO, USA, in 1992 and 1994, respectively, and the Ph.D. degree from the University of Washington, Seattle, WA, USA, in 2000. He is currently an Associate Professor with the Department of Computer Engineering, Kuwait University, Kuwait City, Kuwait, where his interests include analysis/design of computer communication networks. His most recent research emphasis areas include wireless networks, combinatorics, graph theory, control and communication design, optimization in WDM networks, stochastic performance evaluation, and queuing analysis.

Nasro Min-Allah very successfully wears many hats. Currently he is affiliated with the SuperTech group at the Computer Science and Artificial Intelligence Laboratory (CSAIL) at the Massachusetts Institute of Technology (MIT), Boston, MA, where he is a Visiting Scientist. In addition, he is also an Associate Professor and Head of the Department of Computer Science at COMSATS Institute of Information Technology, Pakistan, and Director of its Green Computing and Communication Laboratory. He received his undergraduate and Masters degrees in electronics and information technology in 1998 and 2001, respectively, from Quaid-i-Azam University and Hamdard University, Pakistan. Subsequently, he obtained his Ph.D. in real-time and embedded systems from the Graduate University of the Chinese Academy of Sciences (GUCAS), China, in 2008. His research interests include pipeline parallelism, green computing, chromatic scheduling, and real-time systems.

Ming Peng is a Professor in the Computer Science Department at Wuhan University, Wuhan, China. She received her B.Sc in applied physics and M.S. in computer applications from Wuhan University. She also received her Ph.D. in computer software and theory from Wuhan University. From 2009 to 2011 she was a visiting faculty member in the Electrical and Computer Engineering Department at the University of New Mexico. Currently, Dr. Peng is serving as the Vice President of the Chinese National Multimedia Software Technology Research Center. To date, she has organized and participated in many key projects funded by the Chinese National Natural Science Fund. In addition, she has also participated in two optical-networking projects funded by the US National Science Foundation and US Department of Energy. She was also the technical committee chair of the 2011 IEEE INFOCOM Workshop on High Speed Networks, and her current research interests include network services, performance evaluation, information processing, and distributed computing.

Nasir Ghani is a Professor in the Electrical Engineering Department at the University of South Florida. Earlier he was a faculty member and Associate Department Chair in the ECE Department at the University of New Mexico. He has also spent over 8 years in industry working at several large hi-tech corporations (including Nokia, IBM, and Motorola) and several startups. Currently he is involved in a range of research activities in the areas of cyberinfrastructure design, disaster recovery, cloud computing, and cyber-physical systems (integrated power grids). His research has been supported by the National Science Foundation, Defense Threat Reduction Agency, Department of Energy, Qatar Foundation, Department of Education, NSWC, and Sprint-Nextel Corporation. He also received the NSF CAREER Award in 2005 for his work in multi-domain networking. Dr. Ghani has chaired the IEEE ComSoc Technical Committee on High Speed Networks from 2008 through 2010 and has been a symposium co-chair for IEEE GLOBECOM, IEEE ICC, and IEEE ICCCN. He has also run a workshop series for IEEE INFOCOM and has served on numerous NSF, DoE, and international panels. He is an Associate Editor for *IEEE Systems* and has also served on the editorial board of *IEEE Communications Letters*. He received the Ph.D. degree in computer engineering from the University of Waterloo, Canada.